Ultrasound in Med. & Biol., Vol. 43, No. 9, pp. 1888–1896, 2017

0301-5629/$ - see front matter

http://dx.doi.org/10.1016/j.ultrasmedbio.2017.04.014

● *Original Contribution*

ACOUSTICALLY ACTIVE CATHETER FOR INTRACARDIAC NAVIGATION BY COLOR DOPPLER ULTRASONOGRAPHY

Minako Katayama,* David Zarbatany,† Stephen S. Cha,‡ Mostafa Fatemi,§ and Marek Belohlavek*

*Department of Cardiovascular Diseases, Mayo Clinic, Scottsdale, Arizona, USA; †Independent Engineering Consultant, Laguna Niguel, California, USA; ‡Department of Biostatistics, Mayo Clinic, Scottsdale, Arizona, USA; and §Department of Physiology and Biomedical Engineering, Mayo Clinic, Rochester, Minnesota, USA

(*Received* 17 *November* 2016; *revised* 10 *April* 2017; *in final form* 19 *April* 2017)

Abstract—Navigation of intracardiac catheters by echocardiography is challenging because of the fundamental limitations of B-mode ultrasonography. We describe a catheter fitted with a piezoelectric crystal, which vibrates and produces an instantaneous marker in color flow Doppler scans. The navigation learning curve was explored first in six pigs. Accuracy and precision of targeting with the navigation marker "off" (*i.e.*, B-mode imaging) and "on" were assessed in another six pigs. Paired comparisons confirmed significantly ($p = 0.04$) shorter mean distances achieved in each pig with the color Doppler marker. Pooled (mean ± standard deviation) distance of the catheter tip from the target crystal was 5.27 ± 1.62 mm by B-mode guidance and 3.66 ± 1.45 mm by color Doppler marker navigation. Dye injection targeted into the ischemic border zone was successful in 8 of 10 pigs. Intracardiac catheter navigation with color Doppler ultrasonography is more accurate compared with conventional guidance by B-mode imaging. (E-mail: belohlavek.marek@mayo.edu) © **2017 World Federation for Ultrasound in Medicine & Biology.**

Key Words: **Acoustically active catheter, Color flow Doppler ultrasonography, Ultrasonographic navigation, Ultrasound.**

INTRODUCTION

Ultrasonography of the heart is well established for analysis of cardiovascular function and morphology. Now echocardiography is emerging as a means of navigation during cardiovascular procedures (Lee and Naqvi 2013; Zamorano et al. 2011), especially with the advent of real-time 3-D echocardiography. Practical examples include guidance for pericardiocentesis and navigation for catheter-based intracardiac devices or valves.

The fundamental properties and limitations of B-mode ultrasound signal propagation, such as attenuation, reflection, refraction, scattering and noise, can make reliable identification and navigation of minimally invasive procedures challenging. Therefore, several ultrasonographic methods for navigation of minimally invasive procedures were proposed, and we discussed them in detail elsewhere (Belohlavek et al. 2014). Briefly, one group of techniques is based on a transponder principle and was used for ultrasound-guided placement of minimally invasive instruments, including catheters (Landzberg et al. 1988; Langberg et al. 1988; Vilkomerson and Lyons 1997) or needles (Winsberg et al. 1991). Such a minimally invasive instrument is typically furnished at its tip with a piezoelectric element. However, besides acoustical communication between the instrument and transducer, there is also customization of the ultrasonographic imager circuitry and direct electrical connection required between the piezoelectric element driving unit and the ultrasonographic system. A similar transponder-based approach was adopted for ultrasonographic needle navigation using a sensor formed at the needle tip by co-polymer or piezoelectric coating (Lu et al. 2014). A second group of methods is based on generating a pattern for tracking the instrument in color Doppler scans. For example, a piezoelectric element operating in a passive impedance switching mode has been used to produce localized periodic "flashes" for detection of implanted devices by ultrasound color Doppler (Mari et al. 2013). Other investigators

Address correspondence to: Marek Belohlavek, Department of Cardiovascular Diseases, Mayo Clinic, 13400 East Shea Boulevard, Scottsdale, AZ 85259, USA. E-mail: belohlavek.marek@mayo.edu

(Armstrong et al. 2001; Fronheiser et al. 2008) visualized biopsy needles in color Doppler images through mechanical vibrations induced by a piezoelectric element placed at the needle base and producing a Doppler shift. A third group of approaches benefits from ultrasound signal or image filtering and enhancement, such as in automatic needle detection and tracking in 3-D ultrasound images (Zhao et al. 2013). Ultrasonic needle tracking through coded excitation of the transmitted navigation signal has been proposed recently (Xia et al. 2016) and holds the promise of considerably increasing the signal-to-noise ratio for needle detection in B-mode images.

We previously reported on an intracardiac catheter prototype and guidance of its tip by pulsed-wave (PW) Doppler ultrasonography *in vitro* (McMahon et al. 2012) and *in vivo* (Belohlavek et al. 2014). However, PW Doppler tracking was indirect and required user interaction. In this article, we describe a color flow Doppler marker that tracks the tip of a steerable injection catheter prototype directly in real time and without user interaction. The navigation functionality of our approach is based on using an active piezoelectric crystal affixed to the catheter tip, where this crystal is driven by a continuous signal from a waveform generator. We call this type of catheter an acoustically active catheter (AAC). Interaction of the Doppler signal from the ultrasound scanner with the vibrating crystal generates a new acoustic signal. The new acoustic signal produces the real-time color marker for detection and navigation of the catheter tip. Contrary to the previous transponder-based methods (Landzberg et al. 1988; Langberg et al. 1988; Vilkomerson and Lyons 1997; Winsberg et al. 1991), any conventional clinical Doppler ultrasound imaging system can be used here because no modification of its circuitry or physical connection with the waveform generator is needed in our approach. Also, no piezoelectric adapter for vibration with the entire instrument and no special signal or image processing are needed.

The purpose of this study was to introduce the concept of catheter navigation with conventional color flow Doppler scans and test the method qualitatively by guiding the AAC tip toward an ischemic border zone and quantitatively by measuring the shortest achievable distance of the AAC tip to a pre-defined endocardial point target.

METHODS

Acoustically active catheter design

The current AAC design is based on a 9F Unison sheath (Greatbatch Medical, Minneapolis, MN, USA). The sheath features a steerable tip and a handle with a single-handed lockable slide that controls flexion of the tip. Affixed to the tip is a doughnut-shaped piezoelectric ring crystal with an outer diameter of 3.5 mm (Sonometrics, London, ON, Canada) (Fig. 1a). The crystal serves for navigation and has a central hole with a 1.0-mm diameter. Navigation crystal wiring is protected inside the sheath by a 0.9-mm-outer-diameter polyimide conduit, which is exteriorized through a 1.0-mm hole drilled into the handle wall. The wire connects the crystal to a waveform generator (Agilent 33500 B, Agilent Technologies, Loveland, CO, USA), producing a square-wave driving signal with a frequency of 95 to 100 kHz and amplitude of 0.5 to 1.0 V.

The handle has an infusion port and an integrated entry for catheters (Fig. 1b). Inserted through that entry is our custom sliding injection catheter. The distal end of the injection catheter is assembled from a 17-mm-long 20-gauge needle and a 7-cm distal segment made of a 5F flexible polyvinyl tube. A 5F angiographic catheter (Cordis Europa, Roden, Netherlands) trimmed to a 70-cm length forms the body of the injection catheter. The needle can extend up to 10 mm from the tip through the central hole in the ring crystal. The length of the needle extension can be adjusted with markers drawn on the proximal end of the needle catheter. The AAC is the sheath customized with the inner protective tubing and injection catheter and furnished with the navigation crystal at its tip.

Animal procedures

All animal procedures were approved by the Mayo Clinic Institutional Animal Care and Use Committee. We used adult male domestic pigs weighing 58 to 70 kg (mean ± SD, 67 ± 6 kg). The animal experiments were divided into two series: The first was conducted in March 2016 in six pigs, and the second was conducted in July 2016 in another six pigs. The 3-mo gap allowed time for intermediate assessment of the data and for building improved AAC prototypes.

The animal procedures were the same as previously described (Belohlavek et al. 2014). Briefly, anesthesia was induced with intramuscular tiletamine and zolazepam (Telazol), xylazine and glycopyrrolate. After intubation, each pig underwent mechanical ventilation (Narkomed 6000, Draeger, Telford, PA, USA). Anesthesia and analgesia were maintained by inhalation of isoflurane and intravenous fentanyl, respectively.

The right carotid artery was exposed, and a 14F arterial hemostasis introducer sheath (B. Braun Medical, Bethlehem, PA, USA) was inserted and filled with heparin to accommodate placement of the AAC sheath (with a 4.2-mm outer diameter). Aortic pressure was monitored with a high-fidelity catheter (Millar, Houston, TX, USA) placed in the left or right femoral artery, whereas

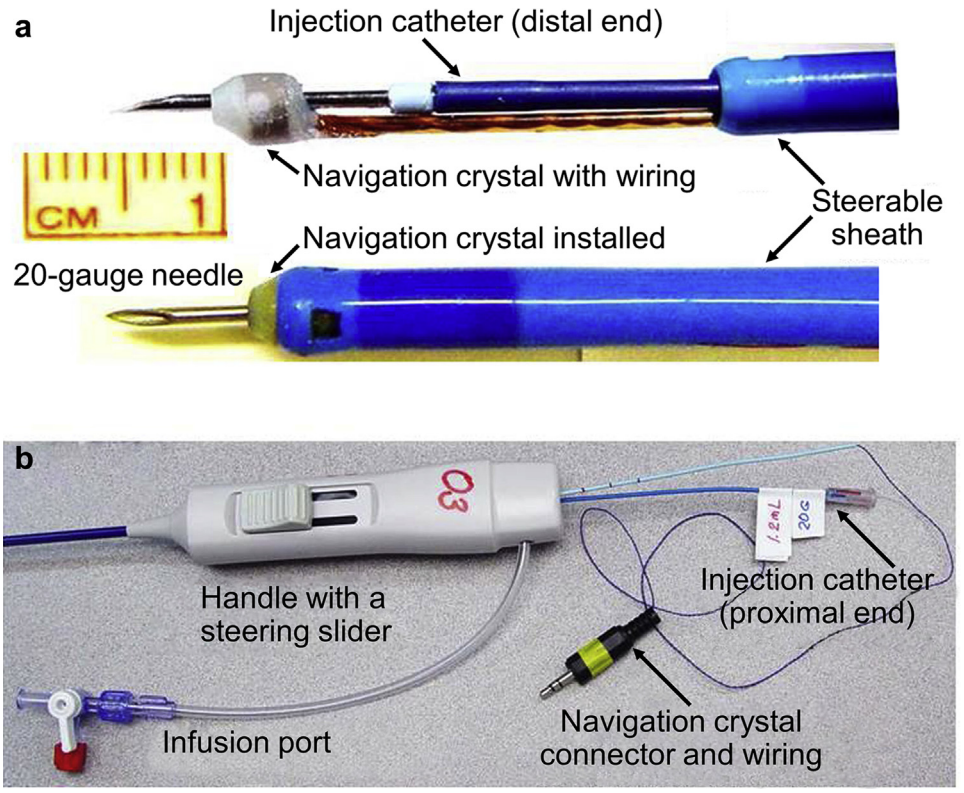

Fig. 1. Acoustically active catheter (AAC) design. (a) AAC tip before and after assembly revealing the ring crystal with its wiring protected by a brown polyimide tube and the distal end of an inner injection catheter (*dark blue*) fitted with a 20-gauge needle. During injection, the needle is extended through a hole in the center of the ring crystal. (b) A handle of the steerable sheath with an exteriorized crystal wire and the proximal end of the injection catheter, including its infusion port.

the left or right femoral vein served as the route for administering fluids and medications. After a median sternotomy was performed, the heart was placed on a pericardial cradle to allow use of instruments and ultrasonography, the pig was heparinized and the AAC was inserted through the hemostasis introducer and placed *via* the aortic valve into the left ventricle.

In the first series of pigs, a portion of the distal left anterior descending coronary artery (length, 2–3 mm) was dissected free of its surroundings, and a snare occluder was placed around the exposed artery to allow on-demand occlusion for pre-conditioning and subsequent permanent occlusion. The ischemic myocardium typically encompassed apical anterior and apical septal myocardial segments. A crystal was implanted into an apical anterior location of the ischemic border zone.

In the second series of pigs, we induced ischemia and implanted a target crystal into the ischemic border zone in the same way as in the first series. However, we also implanted a second endocardial target crystal into the mid-anterolateral left ventricular wall (*i.e.*, outside the ischemic region and border zone) to test targeting in a different location.

Each target crystal was implanted endocardially through a transmyocardial puncture made with thin, pointed forceps, which also aided in proper crystal placement. The crystal was lodged within the endocardial surface, thus effectively plugging the puncture tunnel and creating a point target for navigation tests. The crystal position and its wire were secured, and any residual bleeding was stopped with an epicardial suture.

Transendocardial injection of a green dye bolus (about 0.3 mL of concentrated food color) into the ischemic border zone created a permanent deposit and, thus, marked the anatomic closeness of the injection to the border zone. At the end of each study, a blue dye bolus (32 mL of food color mixed with 8 mL of saline) was injected through the infusion port of the AAC into the left ventricle, and the pig was euthanized with intravenous pentobarbital. The blue dye marked the perfused myocardial region and, thus, visibly delineated the ischemic border zone for analysis by heart dissection during subsequent autopsy.

Ultrasonography and navigation by color Doppler scans

A Vivid 7 (GE Healthcare, Milwaukee, WI, USA) and a GE M4S phased array transducer scanning at 2 MHz were used in this study. During the scans, which were all open-chest scans, a custom polyurethane pad

was interposed between the transducer face and cardiac surface. The pad was calibrated to 8-dB attenuation of a 2-MHz round-trip ultrasonographic signal to approximate attenuation of a human chest wall (Von Bibra et al. 1999).

Contrast ultrasonographic images, which were obtained with 0.5-mL boluses of perflutren lipid microspheres (Definity, Lantheus Medical Imaging, Billerica, MA, USA) followed by a 5-mL saline flush, demarcated the ischemic border zone in a beating heart. The border zone was also estimated by direct visualization of anteroapical epicardial discoloration.

When the AAC tip was within the scan plane, switching from B-mode imaging (Fig. 2a) to color flow Doppler mode displayed a color marker (Fig. 2b). Our method uses a commercially available piezoelectric ring crystal as an active source of an acoustical signal. As a 2-MHz ultrasound beam sweeps across the scan plane, it interacts with the vibrating navigation crystal at the catheter tip. The resulting acoustical interaction produces an elongated color pattern that serves as a marker oriented parallel with the interrogating Doppler beam (Fig. 2b). The color and size of the marker can be adjusted by the frequency and amplitude, respectively, of the acoustical signal transmitted from the crystal. The setting of a color range for measuring flow velocities also affects the appearance of the marker. We used the clinically useful range of 60 to 70 cm/s. With proper adjustment, the color marker appears as a highly localized pointer that is quite practical for rapid and unambiguous identification and tracking of the crystal and, thus, the catheter tip inside the heart.

An important feature of our method is that the acoustical interaction producing the color Doppler marker is strong enough to allow reducing a Doppler gain up to –20 dB, thus considerably subduing or completely eliminating blood flow patterns while still depicting the color marker within the cardiovascular anatomy.

Sonomicrometry

We used 2-mm round sonomicrometric crystals (Sonometrics) for two purposes: (i) These crystals were identifiable on ultrasonography and, therefore, served as endocardial point targets during navigation tests. (ii) A digital ultrasonics measurement system (TRX Series 16, Sonometrics) was connected to the endocardial target crystal and to the crystal at the AAC tip as needed to measure the instantaneous distance between the two crystals. However, the operator was blinded to the actual sonomicrometric distance measurement during each navigation test. Moreover, the navigation tests were performed with the color Doppler marker of the AAC tip turned "on" and "off" to evaluate the guidance effect of the marker compared with conventional B-mode imaging guidance.

In our experimental setting, measuring very short distances (<2 mm) with the sonomicrometric system may result in transmission noise. Short-distance measurements are also limited by the physical size of the piezoelectric crystal. Therefore, we were advised (Wayne Smith, HBSc, Sonometrics, written communication, August 16, 2016) to set the minimum measurable distance to 2 mm to ensure robust results (Fig. 3), although in some targeting tests, the tip of the catheter and the target crystal may have been closer or in direct contact.

Data analysis

For continuous variables, the mean ± SD was used, unless stated otherwise, to describe the instantaneous distance data obtained from sonomicrometric trace samples, which were typically three cardiac cycles long. We also identified the minimal and maximal values in that distance trace sample. All statistical analyses were performed with SAS Version 9.4 software (SAS Institute, Cary, NC, USA), and figures were generated with the R Version 3.3.5 package (R Foundation for Statistical

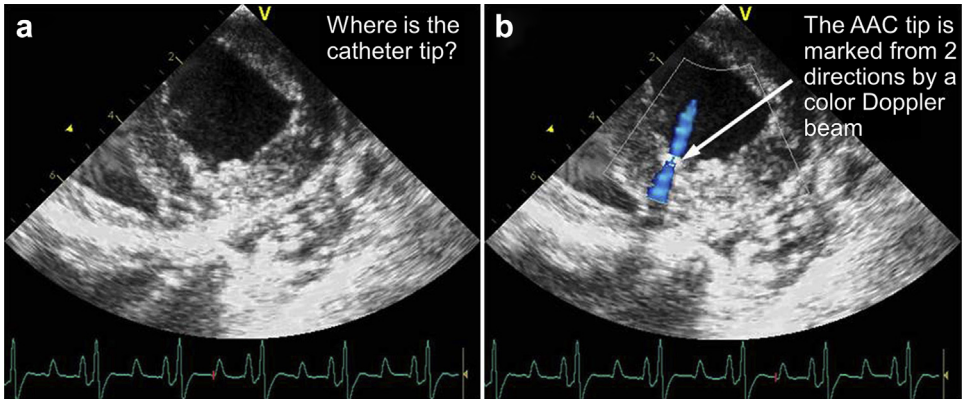

Fig. 2. Real-time color marker. (a) Identification of a catheter in conventional B-mode left ventricular scans can be difficult. (b) The acoustically active catheter (AAC) interacts with a color Doppler beam and produces a color marker (*i.e.*, elongated blue spot in this example). The color marker identifies and tracks the AAC tip in real time as long as the tip is within the scan plane.

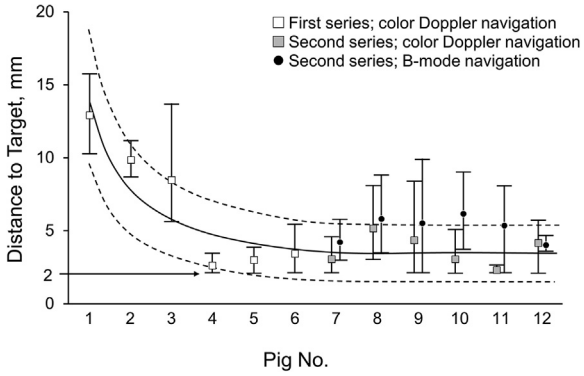

Fig. 3. Learning curve in approaching the target crystal. The data points are the mean values of distance traces from all 12 pigs; the whiskers above and below the means indicate the maximal and minimal values, respectively. Pigs 1 through 6 (*i.e.*, the first series) provided a learning experience with navigation of the acoustically active catheter tip with the color Doppler marker. The *solid line* is the best fit through the mean values with the 1/(pig number) equation, and the *broken lines* on each side of the best fit represent the 95% confidence intervals (CIs) of the means predicted from the best fit. In the second series (pigs 7–12), with color Doppler navigation, the mean distances were within the predicted 95% CIs. With B-mode imaging, however, the mean distances were generally longer, and most were at or outside the 95% CIs. The *arrow* indicates the minimal measurable distance of 2 mm.

Computing, Vienna, Austria). Any p value < 0.05 was considered to indicate statistical significance.

The learning curve with the color flow Doppler navigation was plotted by using the mean and range of the distance (Fig. 3). The means from the six pigs in the first series were analyzed by regression analysis. We considered curve fitting by linear equation, quadratic equation and 1/(pig number). The quotient of 1/(pig number) provided the best fit for expressing the learning curve. We also plotted the 95% confidence interval (CI) of the predicted mean for pigs 1 through 6. We kept the same 95% CI boundary for pigs 7 through 12 (*i.e.*, the second series). If the mean distance from the target for pigs 7 through 12 was within the boundary, it would indicate that the future measurements would be within this expected 95% CI as well.

Distances of the AAC tip to the target achieved in each of the six pigs without the color Doppler marker (Fig. 4a) and with the color marker (Fig. 4b) were traced (Fig. 4, bottom), and their mean ± SD values obtained and plotted (Fig. 5). These paired mean distances were analyzed with a two-sided paired t test. A significantly shorter distance in the paired comparison would indicate a targeting method with higher accuracy. The individual distance measurements from all six pigs were pooled when the Doppler marker was "off" and then when the marker was "on," and a coefficient of variation (*i.e.*, SD/mean) was calculated for each of the two settings to assess precision.

An inter-class correlation coefficient (ICC) (Shrout and Fleiss 1979) was generated in the animals in the second series for assessing the degree of reliability or consistency to which raters with a fixed degree of measurement resemble each other according to the following scale (Cicchetti 1994): poor (ICC $<$0.40); fair ($0.40 <$ ICC < 0.60); good ($0.60 <$ ICC < 0.75); and excellent ($0.75 <$ ICC < 1.00).

RESULTS

Insertion of the AAC into the right carotid artery with the arterial hemostasis introducer sheath was successful in 11 of the 12 pigs. In 1 of the 12 animals, the AAC was inserted *via* the left atrial appendage and secured by a purse string. This alternative access was chosen because both carotid arteries in that pig were too narrow to accommodate the 14F introducer sheath.

Learning curve with color Doppler navigation of the AAC tip

The individual mean, minimal and maximal distances between the AAC tip and the target crystal are illustrated in Figure 3. In the first series (pigs 1–6), the distance between the AAC tip and the target crystal progressively shortened. We achieved an approximately 3.0-mm average distance in the last three tests in this series. In the second series (pigs 7–12), when the color Doppler marker was used, the mean distances were within a 95% CI range, and the minimum value was 2 mm in 5 of the 6 pigs. With B-mode navigation, mean distances in 4 of the 6 pigs were at or outside the 95% CI, and the minimal distance was reached only in 2 pigs.

Navigation of the AAC tip to the target crystal

In each pig in the second series, we performed two navigation tests to the target crystal located in the non-ischemic mid-anterolateral region. In the first test, the color Doppler marker was turned "off" and the catheter tip was guided by B-mode imaging only (Fig. 4a). After pulling the AAC away from the target, we performed a second targeting test but with the color Doppler marker turned "on" (Fig. 4b).

Mean distances to the target were consistently shorter when the color Doppler marker navigation was turned "on" (Fig. 5). The differences in these mean distances were statistically significant ($p = 0.04$) in a paired comparison. The mean ± SD values of data pooled from all 6 pigs for B-mode guidance and for color Doppler marker navigation were 5.27 ± 1.62 and 3.66 ± 1.45 mm, respectively. Coefficients of variation were 0.31 and 0.40, respectively.

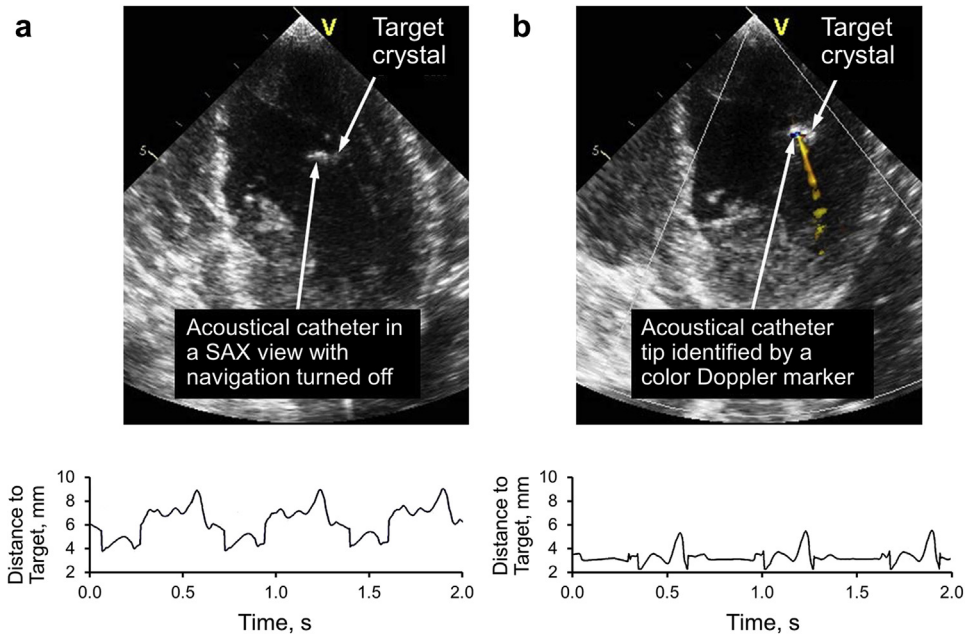

Fig. 4. Navigation to the target crystal. (a) In B-mode navigation of the acoustical catheter without the aid of the color Doppler marker, a short-axis (SAX) view suggests that the catheter is in direct contact with the target crystal, but distances to the target vary from 4 to 8 mm because, based on B-mode navigation only, the tip of the catheter may not be within the scan plane. Thus, the target is hit by the catheter, but not by its tip, as would be desirable. (b) Navigation with the color Doppler marker ensures that the catheter tip is within the scan plane and reliably guided toward the target. In this example, the tip touches the target, which is visible in the captured color Doppler scan and documented by the sonomicrometric trace that periodically, as the heart beats, reaches the minimal measurable distance of 2 mm.

Inter-observer consistency of analyzing distances by sonomicrometry

The sonomicrometric machine settings were kept unchanged throughout the entire study. The resulting ICCs for inter-observer measurements of the sonomicrometry data were 0.996 (95% CI, 0.977–1.000) for distances achieved by B-mode navigation and 1.000 (95% CI, 1.00–1.000) for distance data obtained by color Doppler navigation.

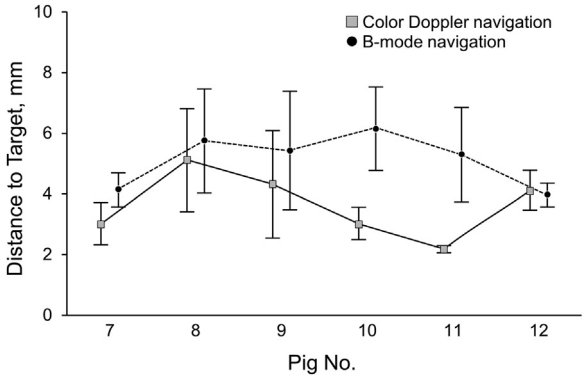

Fig. 5. Distance to the target crystal in the second series of animals. The data points are the mean values of distance traces from the six pigs in the second series; the whiskers represent standard deviations. The approximate range of the mean distances in sonomicrometric traces from navigating the acoustically active catheter tip by B-mode imaging was 4 to 6 mm. Mean distances from navigating by the color Doppler marker were shorter (approximately 2–5 mm). This difference was significant by a paired comparison ($p = 0.04$).

Color dye injection into the ischemic border zone

Targeted transendocardial injections of color dye were attempted in 10 of the 12 pigs. This test was not attempted in the other 2 pigs because of acute perioperative complications. Successful transendocardial injection, defined as a localized intramyocardial deposit of green dye within the ischemic border zone (Fig. 6), was confirmed in 8 of 10 pigs (5 in the first series and 3 in the second series). In 1 of the 10 pigs, the needle perforated the thinned ischemic left ventricular wall near the border zone. In another 1 of the 10 pigs, we could not determine why no green dye was deposited, as discovered at autopsy.

DISCUSSION

This experimental study examined intracardiac navigation of an AAC by conventional color flow Doppler imaging. It expanded on our previous work (Belohlavek et al. 2014; McMahon et al. 2012), in which we interactively identified and tracked a catheter tip with a

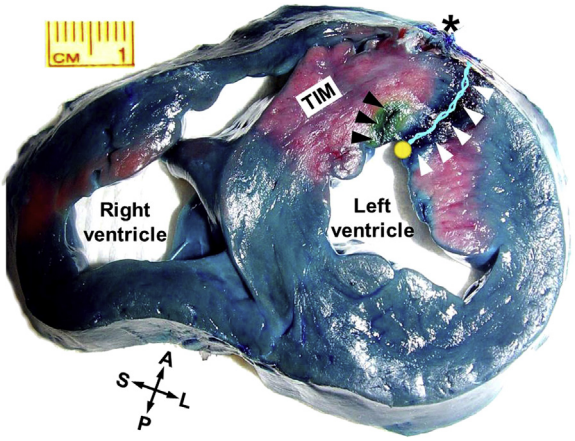

Fig. 6. Ischemic border zone and transendocardial injection on autopsy. *Blue stain* indicates perfused myocardium. The *white arrowheads* indicate an anterior border zone of anteroseptal transmurally ischemic myocardium (TIM). The crystal and its wire were implanted through that border zone; its dark appearance is due to implantation injury. The crystal and wire were removed before heart dissection; therefore, their location is approximated by a drawing. Transmural ischemia was induced by ligating the left anterior descending coronary artery (*asterisk*). The *black arrowheads* point to a green dye deposit made by transendocardial injection after navigating a tip of the acoustically active catheter to the target crystal. A = anterior; L = lateral; P = posterior; S = septal.

PW Doppler sample window. The current work introduces a technically advanced AAC prototype that identifies the catheter tip by a color Doppler marker instantaneously and without the need for user interaction. We found that the color marker navigates the AAC tip to an endocardial point target with higher spatial accuracy than B-mode imaging.

Intracardiac injection catheter guidance

Growing interest in intracardiac delivery of cellular or therapeutic agents led to developments and pre-clinical or clinical tests of steerable injection catheters that can be tracked with magnetic resonance imaging (Karmarkar et al. 2004), electroanatomic mapping (McCall et al. 2012; Minguell et al. 2011) or conventional fluoroscopy. Conceivably, these catheters could be further adapted by a miniature piezoelectric crystal suitable for spatial tracking and navigation by Doppler ultrasonography. However, to avoid logistical, proprietary and technical issues, we decided to base the design of our custom steerable injection catheter prototype on a commercially available Unison sheath (Fig. 1), which is intended for delivery of therapeutic devices into a vascular system. Its steerable distal end, infusion port, integrated entry for catheters and 9F inner diameter provided an excellent developmental platform for pre-clinical tests of the AAC prototype and its color Doppler guidance.

The fundamental properties and limitations of B-mode echocardiography can cause artifacts, such as sparse or blurry depictions of the catheter tip or its visual merging with anatomic surroundings (Fig. 2a). To overcome this problem, we added an active acoustical source (*i.e.*, a vibrating piezoelectric crystal) to the tip of the catheter. In color flow Doppler scans, the crystal produces a color marker (Fig. 2b), which eliminates the undesired ambiguity of visually detecting the catheter tip in B-mode images, as long as the tip is located within the scan plane. However, some learning experience was needed to achieve time-efficient navigation of the AAC tip and minimize the targeting distance.

Learning curve and spatial accuracy of intracardiac navigation to a point target

The learning curve (Fig. 3) features rather long mean distances (*i.e.,* 8–13 mm) to the target crystal in the first 3 pigs. Admittedly, each of these learning tests in the first series also took a relatively long time (about 20–30 min) to properly place and flex the distal end of the AAC to guide its tip toward the endocardial point-target location. In a pig heart, the left ventricular cavity is smaller than that of an adult human heart (*i.e.*, less accommodating for steering with the AAC tip), and its systolic–diastolic cycling leads to a rapid and frequently occurring out-of-plane motion of the AAC tip. Therefore, navigation with the prototype catheter with stiff steering caused by the inner tubing was a real challenge. As we gained practical experience, however, we became more proficient (procedural time, about 10–15 min) in proper intraventricular placement of the AAC and better at aiming the tip toward the target crystal. This is documented by the short mean distance (about 3 mm) and the minimal measurable distance (about 2 mm) in the last 3 animals of the first series (Fig. 3, pigs 4–6).

In the second series of 6 pigs, which we studied after a 3-mo gap, we targeted a crystal that was in a different (mid-anterolateral) left ventricular location. Distances to the target crystal achieved with the use of a color Doppler marker were within a 95% CI range that was expected according to the data from the first series. In addition, most targeting tests (5 of the 6 pigs) achieved the minimal measurable distance, suggesting that the AAC user (M.B.) retained the practical experience. With B-mode navigation only, the inability to identify and guide the catheter tip within a scan plane was reflected by worse targeting performance, as measured by mean and minimal achievable distances. Interpretation of the mean and minimal distances in Figure 3 requires keeping in mind that sonomicrometry is technically limited to measuring distances of at least 2 mm. Therefore, achieving a 2-mm distance was the best measurable result in our study, which was reached with B-mode navigation in only 2 of 6 pigs.

Other investigators (Landzberg et al. 1988) tested spatial accuracy of a prototype transponder catheter system in a similar experimental setting by targeting the tricuspid annulus and fossa ovalis. Direct measurements of a radiofrequency lesion at autopsy revealed that the transponder catheter tip ended 2.8 ± 0.7 mm from the edge of the lateral tricuspid annulus and 3.5 ± 3.1 mm from the center of the fossa ovalis. With our color Doppler marker navigation, we achieved a distance of 3.66 ± 1.45 mm, which corresponds closely to those results despite approaching a considerably moving endocardial point target in our setting.

Conventional B-mode versus proposed color Doppler navigation

The experimental catheter was mostly identifiable in B-mode images, as it is in clinical scans. However, there was no assurance with gray-scale visual navigation that the tip was interrogated by the B-mode imaging plane and properly guided to the target. Thus, the main benefits of using the color Doppler marker on the AAC tip are (i) verification that the AAC tip is within the scan plane and (ii) real-time guidance of the tip toward the target crystal (Fig. 4). This verification and instantaneous guidance of a moving AAC tip toward the moving target in the beating heart were, in our opinion, the main factor in achieving consistently closer mean navigation distances (*i.e.*, higher accuracy) in individual animals with the color Doppler marker compared with B-mode navigation (Fig. 5). The coefficient of variation with the color marker "on" was slightly higher compared with that with the color marker "off" (*i.e.,* B-mode navigation only) because the overall mean distance to the target achieved with the color Doppler marker was shorter than that with B-mode, but the variability, expressed by the SD of distance measurements, did not drop proportionally. The variability was influenced mainly by the cyclic motion of a beating heart, the rate and magnitude of which were similar in both navigation settings.

During each targeting test, when the AAC user felt that the AAC tip had approached the target as closely as possible, navigation by the color Doppler marker was disconnected, and the reference sonomicrometric tracing of the actual targeting distances was recorded. Any theoretical subjectivity in off-line evaluation of sonomicrometric measurement cycles by the two independent users (M.B. and M.K.) was essentially nonexistent, as documented by the high ICC values (*i.e.,* excellent consistency between the two raters), for both B-mode and color flow Doppler navigation approaches.

Dye injection targeted to an ischemic border zone

Deployment of a needle for transendocardial injection of green dye simulated intramyocardial deposition of an investigative or therapeutic agent. These tests were a continuation of our previous work (Belohlavek et al. 2014), in which we used interactive PW Doppler navigation and initially experimented with intracardiac injections of a dye into ischemic myocardium. In the present study, we not only used the newly proposed real-time color Doppler marker, but also chose a more challenging target—an ischemic border zone. We defined, by placement of a piezoelectric crystal, a specific endocardial point target within the border zone. The reason for such a specific target was twofold: (i) The border zone can span several centimeters and thus form a rather ambiguous target; and (ii) the target crystal in the border zone was used for an independent sonomicrometric measurement of a distance between the AAC tip and the target. The green dye deposit then confirmed guidance to the border zone anatomically (Fig. 6), and successful targeted transendocardial injections for 8 of 10 pigs suggested proper functionality of the injection catheter prototype.

Clinical relevance and practical perspectives

Emerging or existing minimally invasive intracardiac interventions require highly accurate spatial guidance toward a target within a beating heart and highly accurate anatomic depictions. The AAC in combination with a broadly available, portable and non-ionizing Doppler imaging technology fulfills that requirement. This system is cost efficient: (i) Our method does not require the hardware modifications of a conventional color flow Doppler ultrasound system. (ii) Piezoelectric crystals are inexpensive and readily available in various sizes and shapes. (iii) The required square-wave signal that drives vibrations of the crystal at the AAC tip might be generated by a low-cost integrated circuit that could be designed to fit into the catheter handle and be powered by a small battery.

From a broader perspective, the current approach could be used for navigation with any minimally invasive instrument as long as such an instrument allows attachment of a piezoelectric crystal and the location of an anatomic target is within the acoustical reach of ultrasound imaging. Our future efforts will aim at designing an even more compact acoustical tip for the catheter and exploring options for more control over the shape and size of the navigation color Doppler marker.

Limitations

The navigation color marker is a result of an acoustical interaction between the crystal vibrating at the AAC tip and the interrogating Doppler beam. The color, intensity and size of the marker, as well as subduing the surrounding blood flow patterns, are controlled by the frequency and amplitude of the crystal vibrations and

by the velocity range and gain settings of the color flow Doppler imaging system. But the navigation marker shape (Figs. 2b and 4b) (*i.e.,* an elongated color spot pointing at the AAC tip along the interrogating beam direction) is determined by beamforming of the ultrasound machine. This is a trade-off for the ability to use any Doppler ultrasound system without any modification of its circuitry or connection with the waveform generator that controls the navigation crystal.

Our present study was based on 2-D scans. However, the color Doppler marker also works in a 3-D format, as we preliminarily verified *in vitro* with a 3-V transducer (GE Healthcare). Slow image rate during 3-D color flow Doppler scans was the main reason we resorted to 2-D imaging in the present study with beating pig hearts. Targeting was anatomically limited to the apical anterior (*i.e.,* ischemic border zone) and mid-anterolateral regions of the left ventricle. The basal regions were not accessible because the sheath flexing was restricted by the material available to us for manufacturing the inner protective conduit and injection catheter tubing. The posterior wall was not targeted because access would be difficult for target crystal implantation, and the septal wall was not targeted because target crystal placement would require puncturing the right ventricular wall.

CONCLUSIONS

Minimal distances of 2 mm from a pre-defined endocardial point target, which were achieved by guiding the acoustically active catheter tip with a color Doppler marker, illustrate better spatial navigation accuracy inside the beating left ventricle compared with guidance of the catheter by conventional B-mode ultrasound imaging. This experimental study is a developmental step toward a novel use of broadly clinically available color flow Doppler ultrasonography for navigation of minimally invasive cardiovascular procedures.

Acknowledgments—We thank Gillian Murphy for administrative help and Naomi M. Gades, DVM, MS, and Jillian C. Dworaczyk, CVT, for extensive veterinary assistance. The Unison steerable sheaths were provided for prototyping by Greatbatch Medical. This study was funded by R01 Grant EB019947 from the National Institutes of Health. The contents of the study are solely the responsibility of the authors and do not necessarily represent the official views of the National Institutes of Health.

REFERENCES

Armstrong G, Cardon L, Vilkomerson D, Lipson D, Wong J, Rodriguez LL, Thomas JD, Griffin BP. Localization of needle tip with color Doppler during pericardiocentesis: in vitro validation and initial clinical application. J Am Soc Echocardiogr 2001;14:29–37.

Belohlavek M, Katayama M, Zarbatany D, Fortuin FD, Fatemi M, Nenadic IZ, McMahon EM. Acoustically active injection catheter guided by ultrasound: Navigation tests in acutely ischemic porcine hearts. Ultrasound Med Biol 2014;40:1650–1659.

Cicchetti DV. Guidelines, criteria, and rules of thumb for evaluating normed and standardized assessment instrument in psychology. Psychol Assess 1994;6:284–290.

Fronheiser MP, Idriss SF, Wolf PD, Smith SW. Vibrating interventional device detection using real-time 3-D color Doppler. IEEE Trans Ultrason Ferroelectr Freq Control 2008;55:1355–1362.

Karmarkar PV, Kraitchman DL, Izbudak I, Hofmann LV, Amado LC, Fritzges D, Young R, Pittenger M, Bulte JW, Atalar E. MR-trackable intramyocardial injection catheter. Magn Reson Med 2004;51:1163–1172.

Landzberg JS, Franklin JO, Langberg JJ, Herre JM, Scheinman MM, Schiller NB. The transponder system: A new method of precise catheter placement in the right atrium under echocardiographic guidance. J Am Coll Cardiol 1988;12:753–756.

Langberg JJ, Franklin JO, Landzberg JS, Herre JM, Kee L, Chin MC, Bharati S, Lev M, Himelman RB, Schiller NB, Griffin JC, Scheinman MM. The echo-transponder electrode catheter: A new method for mapping the left ventricle. J Am Coll Cardiol 1988;12:218–223.

Lee MS, Naqvi TZ. A practical guide to the use of echocardiography in assisting structural heart disease interventions. Cardiol Clin 2013;31:441–454.

Lu H, Li J, Lu Q, Bharat S, Erkamp R, Chen B, Drysdale J, Vignon F, Jain A. A new sensor technology for 2-D ultrasound-guided needle tracking. Med Image Comput Comput Assist Interv 2014;17(Pt 2):389–396.

Mari JM, Lafon C, Chapelon JY. Detection of deeply implanted impedance-switching devices using ultrasound Doppler. IEEE Trans Ultrason Ferroelectr Freq Control 2013;60:1074–1083.

McCall FC, Telukuntla KS, Karantalis V, Suncion VY, Heldman AW, Mushtaq M, Williams AR, Hare JM. Myocardial infarction and intramyocardial injection models in swine. Nat Protoc 2012;7:1479–1496.

McMahon EM, Jiamsripong P, Katayama M, Chaliki HP, Fatemi M, Belohlavek M. Accurate guidance of a catheter by ultrasound imaging and identification of a catheter tip by pulsed-wave Doppler. Pacing Clin Electrophysiol 2012;35:44–50.

Minguell JJ, Lorino R, Lasala GP. Myocardial implantation of a combination stem cell product by using a transendocardial MYOSTAR injection catheter: A technical assessment. Acute Card Care 2011;13:40–42.

Shrout PE, Fleiss JL. Intraclass correlations: Uses in assessing rater reliability. Psychol Bull 1979;86:420–428.

Vilkomerson D, Lyons D. A system for ultrasonic beacon-guidance of catheters and other minimally-invasive medical devices. IEEE Trans Ultrason Ferroelectr Freq Control 1997;44:496–504.

Von Bibra H, Voigt JU, Froman M, Bone D, Wranne B, Juhlin-Dannfeldt A. Interaction of microbubbles with ultrasound. Echocardiography 1999;16(7 Pt 2):733–741.

Winsberg F, Mitty HA, Shapiro RS, Yeh HC. Use of an acoustic transponder for US visualization of biopsy needles. Radiology 1991;180:877–878.

Xia W, Ginsberg Y, West SJ, Nikitichev DI, Ourselin S, David AL, Desjardins AE. Coded excitation ultrasonic needle tracking: An in vivo study. Med Phys 2016;43:4065.

Zamorano JL, Badano LP, Bruce C, Chan KL, Goncalves A, Hahn RT, Keane MG, La Canna G, Monaghan MJ, Nihoyannopoulos P, Silvestry FE, Vanoverschelde JL, Gillam LD. EAE/ASE recommendations for the use of echocardiography in new transcatheter interventions for valvular heart disease. J Am Soc Echocardiogr 2011;24:937–965.

Zhao Y, Cachard C, Liebgott H. Automatic needle detection and tracking in 3-D ultrasound using an ROI-based RANSAC and Kalman method. Ultrason Imaging 2013;35:283–306.